Density Functional Theory Investigation into the Stereocontrol of the Syndiospecific Polymerization of Propylene Catalyzed by C_s-Symmetric Zirconocenes

Simone Tomasi,[†] Abbas Razavi,[‡] and Tom Ziegler*,[†]

Department of Chemistry, University of Calgary, 2500 University Drive NW, Calgary, Alberta, Canada T2N 1N4, and Total Petrochemicals Research Feluy, Zone Industrielle C, B-7181 Seneffe (Feluy), Belgium

Received August 29, 2006

The mechanisms of the two most likely routes for the generation of stereodefects in the syndiospecific polymerization of propylene, mediated by the C_s-symmetric *ansa*-zirconocenes $Me_2CCpFluZrR^+X^-$ (**1**), $Me_2CCp(3,6\text{-di-Me-Flu})ZrR^+X^-$ (**2a**), $Me_2SiCp(3,6\text{-di-Me-Flu})ZrR^+X^-$ (**2b**), and $Me_2CCp(3,6\text{-di-tBu-Flu})ZrR^+X^-$ (**3**) ($X^- = MeB(C_6F_5)_3^-$, $FAl(Bip_f)_3^-$, $MAOMe^-$) are explored using density functional theory. Site epimerization events (also known as back-skip or missed insertion) generate defective single *m* dyads, while enantiomeric misinsertions are the main source of double *mm* triads. The most important factor affecting the frequency of enantiomeric misinsertion is the structure of the ligand, while the counterion and solvation have little effect. Site epimerization is also influenced by the nature of the ligand system, but the bulk and the charge distribution of the anion are more prominent factors. The inclusion of solvent effects in the modeling of the site epimerization is critical for explaining reactivity and to achieving at least qualitatively correct results. Application of the two-parameter probabilistic scheme developed by Farina and co-workers allows for the prediction of pentad distributions from the computed selectivities. The good agreement found between experiment and computations for the basic unsubstituted system invented by Ewen and Razavi validates the proposed model. Thus, the computed pentad distributions may be used for assessing the effectiveness of modifications to the ligands on syndioselectivity. Increasing the bulk of 3,6-substituents on the fluorenyl ligand leads to increased syndiotacticity, without significantly affecting the reactivity. By introducing a stereogenic center on the alkyl chain, it is possible to assess the influence of chain end control on stereoselectivity. The main effect of chain end control is to increase the stereoselectivity after a stereoerror.

Introduction

Complete control over physical, mechanical, and thermal properties of polymers is an absolute requirement for the design of polymeric materials that have the right characteristics appropriate for a wide variety of applications.

A revolution in olefin polymerizations was started with the advent of homogeneous metallocene catalysts from the early 1980s.[1−3] Single-site systems, with well-defined catalytic centers, have allowed a much better understanding of the polymerization mechanism and its underlying forces.[4,5] These early breakthroughs opened the possibility for rationally modifying the ligand structure, thus affording increased control over polymer properties, as well as widening and deepening the understanding of the fine details in the polymerization process.[6−10] A great deal of information has been accumulated, as the result of both experimental and theoretical studies on the olefin polymerization mechanism, on the side reactions, and on the effect the structure of the ligand and the counterion has on reactivity and stereoselectivity.

Metallocene catalysts are in many ways a more attractive industrial alternative to traditional Ziegler−Natta systems. This is due to the high degree of control they allow over average molecular weight, molecular weight distribution, and tacticity (and therefore thermal and mechanical properties).

Progress in the control of polymer properties through catalyst design has continued, but there still is room for further advances. For example, while highly isotactic polypropylene is obtained quite easily, the syndiotactic polymerization of propylene is not as efficient and would benefit from optimization of the catalyst stereoselectivity. Furthermore, catalytic systems for syndiotactic polymerizations are intrinsically interesting, as they offer opportunities for testing the theories on catalyst symmetry−stereocontrol relationships.[11] It is well-known that the local symmetry of the catalyst dictates the stereoselectivity of the polymerization.[12] Systems for the isospecific polymerization of olefins are either C_2 symmetric, with homotopic catalytic sites,

[†] University of Calgary.
[‡] Total Petrochemicals Research Feluy.

(1) Ewen, J. A. *J. Am. Chem. Soc*. **1984**, *106*, 6355.
(2) Kaminski, W.; Kulper, H.; Britzinger, H. H.; Wild, F. R. W. P. *Angew. Chem., Int. Ed. Engl.* **1985**, *24*, 507.
(3) Ewen. J. A.; Jones, R. L.; Razavi, A.; Ferrara, J. D. *J. Am. Chem. Soc*. **1988**, *110*, 6255.
(4) Ewen. J. A.; Jones, R. L.; Curtis, S.; Cheng, H. N. In *Catalytic Olefin Polymerization*; Keii, T., Soga, K., Eds.; Elsevier: New York, 1990; p 439.
(5) Ewen. J. A.; Elder, M. J.; Jones, R. L.; Haspeslagh, L. Atwood, J. L. *Makromol. Chem. Makromol. Symp.* **1991**, *48−49*, 253.
(6) Britzinger, H. H.; Fischer, D.; Mülhaupt, R.; Rieger, B.; Waymouth, R. *Angew. Chem., Int. Ed. Engl.* **1995**, *34*, 1143.
(7) Scheirs, J., Kaminski, W., Eds. *Metallocene-Based Polyolefins*; Wiley: Chichester, U.K., 2000; Vols. 1 and 2.
(8) Alt, H. G.; Köppl, A. *Chem. Rev.* **2000**, *100*, 1205.
(9) Resconi, L.; Cavallo, L.; Fait, A.; Piemontesi, F. *Chem. Rev.* **2000**, *100*, 1253.
(10) Chen, E. Y. X.; Marks, T. J. *Chem. Rev.* **2000**, *100*, 1391.
(11) Di Silvestro, G.; Sozzani, P.; Terragni, A. *Macromol. Chem. Phys*. **1996**, *197*, 3209.
(12) Ewen. J. A. *J. Mol. Catal. A* **1998**, *128*, 103.

10.1021/om060786v CCC: $37.00
Publication on Web 03/07/2007

Scheme 1. Mechanisms of the Enantiofacial Misinsertion and of the Site Epimerization and Their Signature in the Pentad Distribution

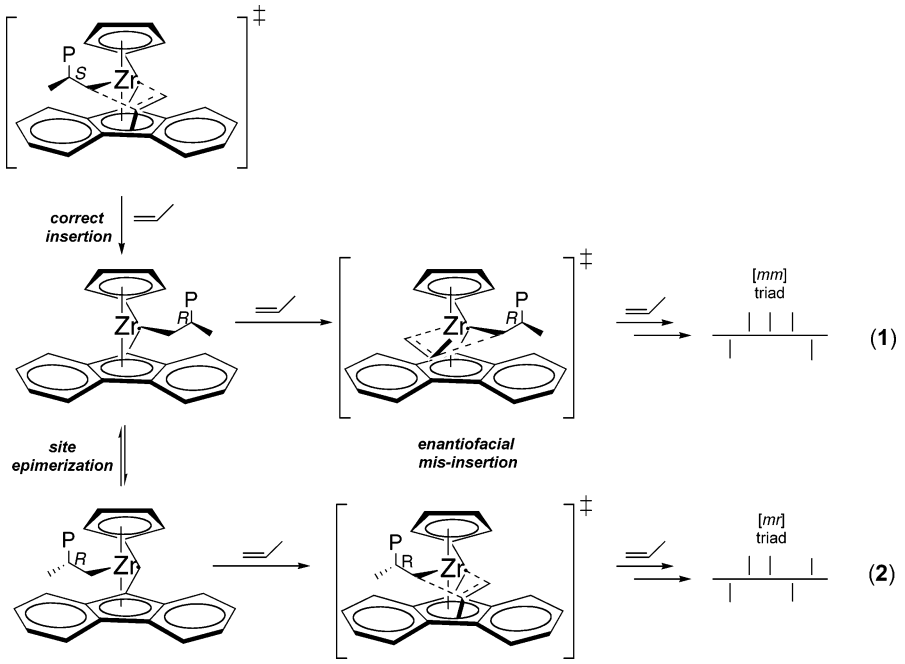

or C_1 symmetric, with heterotopic sites. In the latter case, usually only a single coordination site is made available after substituting one side of a C_s-symmetric system with bulky groups. These two classes of catalysts do not allow for the detection of errors in the alternation of the coordination site, which is proposed by the widely accepted Cossee mechanism.[13−15] In the first system this is because the two sites are equivalent, while in the second system one site is deliberately blocked so that alternation is not possible. There are cases in which site epimerization has been detected in C_1-symmetric systems,[16] and this has led to question the hypothesis that one of the two coordination sites is completely blocked by the bulky substituent.[17] Isotactic polymers are therefore not affected by the so-called site epimerization (also known as chain back-skip, or missed insertion) as a source of stereoerrors, whereas such a process affects syndiotactic polymers, which are most commonly generated by C_s-symmetric systems.

It is commonly accepted that the single main source of stereoerrors in the syndiospecific polymerization of propylene is enantiomeric misinsertion: i.e., the insertion of a monomer unit with the "wrong" enantioface. The "right" enantioface would be the one that allows minimization of repulsive steric interactions between the olefin side group and the growing polymer chain, as well as between the ligands and the growing polymer chain. This is best attained when the olefin substituent and the alkyl chain are in an anti relationship, while at the same time the alkyl chain is as far away as possible from the bulkier of the ligands. An enantiomeric misinsertion (EMI) event in the syndiotactic polymerization of propylene leads to the occurrence of an *mm* triad error, as depicted in Scheme 1, whereas a perfect syndiotactic polymer is composed exclusively of racemic *r* dyads.

In contrast, a site epimerization (SE) event leads to the occurrence of a single *m* dyad error. A SE event occurs when the alkyl chain moves to an empty coordination site before a monomer unit is taken up (see Scheme 1). This event can in principle take place in two ways, with or without the assistance of the counterion, and its rate is independent of the concentration of the monomer. All insertion processes, on the other hand, are bimolecular and their rates depend on both the concentration of the catalyst and the monomer. Therefore, it can be inferred that the incidence of SE relative to EMI is higher at low monomer concentrations, and this is indeed observed experimentally. A single *m* dyad error can also be obtained when the monomer coordinates opposite to the anion (trans attack or "back-side attack"),[18] rather than attacking from the same side (cis), in which case no dependence on monomer concentration should be observed. It is widely accepted that cis coordination is kinetically favored, but it is possible that the "back-side" attack concurs in generating single *m* dyad errors. However, on the basis of experimental kinetics studies, site epimerization seems to be a more likely source. Computational studies also seem to suggest that the "back-side attack" is not an effective source for single *m* dyad errors.[19,20]

It is important to understand how misinsertion and site epimerization events occur, because understanding their origins is the key to discovering how to minimize them. At this stage, the insight provided by molecular modeling and especially by accurate quantum chemical calculations brings an invaluable contribution. Numerous computational works, from the early 1990s on, have dealt with the subject of olefin polymerizations in general and with the control of stereochemistry in particular. Early studies by Corradini et al.,[21−24] as well as Rappé et al.,[25−27] have provided the first rationalization of the stereochemistry

(13) Cossee, P. *J. Catal*. **1964**, *3*, 80.
(14) Arlman, E. J.; Cossee, P. *J. Catal*. **1964**, *3*, 99.
(15) Cossee, P. In *Stereochemistry of Macromolecules*; Ketley, A. D., Ed.; Dekker: New York, 1967; Vol. 1, Chapter 3.
(16) Rieger, B.; Jany, G.; Fawzi, R.; Steimann, M. *Organometallics* **1994**, *13*, 647.
(17) Miller, S.; Bercaw, J. E. *Organometallics* **2006**, *25*, 3576.
(18) Chen, M.-C.; Roberts, J. A. S.; Marks, T. J. *J. Am. Chem. Soc.* **2004**, *126*, 4605.
(19) Borrelli, M.; Busico, V.; Cipullo, R.; Ronca, S.; Budzelaar, P. H. M. *Macromolecules* **2003**, *36*, 8171 and ref 4b therein.
(20) Lohrenz, J. C. W.; Woo, T. K.; Fan, L.; Ziegler, T. *J. Organomet. Chem.* **1995**, *497*, 91.
(21) Corradini, P.; Guerra, G.; Vacatello, M.; Villani, V. *Gazz. Chim. Ital*. **1988**, *118*, 173.

of insertion. Their conclusions, based on results obtained from force-field calculations, have been further developed by others but stand to our day essentially unchanged in their essence. Many other computational groups have since contributed to virtually all aspects of the olefin polymerization process, including detailed structural and energetic characterization of the intermediates involved in the reaction mechanism,[28,29] the role of the solvent and of the counteranion,[30−36] stabilizing agostic interactions, side reactions (leading to chain branching and termination),[37,38] regioselectivity, and stereoselectivity.[39−42]

The focus of this paper is on the factors that contribute to stereocontrol in the syndiospecific polymerization of propylene, catalyzed by systems belonging to the class of C_s-symmetric, single-site homogeneous catalysts discovered by Ewen and Razavi. We are interested in knowing how the size of increasingly large substituents on the fluorenyl ligand affects enantioface selectivity. Furthermore, considerable efforts have been invested to find a convincing description of the mechanism of site epimerization. The literature concerning computational investigations into the mechanism of site epimerization is in fact scarce, and to our knowledge no one has yet accurately described the critical role played by the counterion in this process.[43]

Computational Details

Density functional theory (DFT) calculations on the systems of interest were carried out with the program ADF,[44,45] version 2005.01,[46] using the Becke−Perdew exchange-correlation functional (BP86).[47−49]

Double-ζ STO basis sets with a polarization function were employed for the H, B, C, O, Al, Si, and Cl atoms, while for the Zr atom a triple-ζ STO basis set with one p-type polarization function was employed. The 1s electrons of B, C, and O as well as the 1s−2p electrons of Al and Si and the 1s−3d electrons of Zr were treated as frozen core. First-order scalar relativistic corrections were applied to the systems studied.[50−52]

Chart 1. Types of C_s-Symmetric Systems Studied in This Investigation

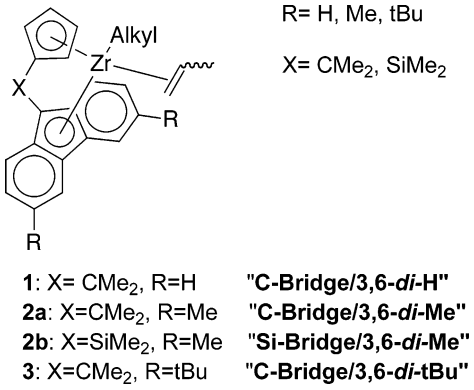

All optimizations were carried out in the gas phase without any symmetry constraint.

For the insertion of propylene into the Zr−alkyl bond, approximate transition states were located through reaction coordinate studies in which all degrees of freedom were minimized, while keeping fixed the C−C separation in the bond being formed. In the metallocene-catalyzed polymerization of olefins, the anion plays a fundamental role in determining the reaction rate, because of the high activation energy required to extract the anion from the ion pair to free a metal site for monomer uptake. However, the magnitude of the effect is the same for the correct insertion and for misinsertion; therefore, when the relative rate of enantiomeric misinsertion is studied, the anion can be disregarded. DFT calculations performed in our group have shown that the stereoselectivity changes minimally (∼0.1 kcal/mol) when the anion is included, proving that this approximation is justified.[53] All stationary points were then fully optimized as minima or transition states, starting from the constrained geometries. Transition states were characterized as having a single imaginary frequency. Frequency calculations have yielded a very high number of low-frequency modes. Under these conditions the harmonic oscillator approximation, under which vibrational frequencies are calculated, fails, thus affording unreliable values for the corrections to Gibbs free energies. For this reason reaction energies and not free energies are reported throughout the paper.

For the site epimerization the counteranion plays a fundamental role; therefore, it must be included in the description. Due to the very large size of the system and the high number of ligand−anion combinations, it has been necessary to resort to a hybrid QM/MM description. Hybrid quantum-mechanical (QM) and molecular-mechanical (MM) models (QM/MM) have been applied to the geometry optimizations that included the anion, using the IMOMM scheme by Morokuma and Maseras,[54] as implemented in ADF by

(22) Cavallo, L.; Guerra, G.; Oliva, L.; Vacatello, M.; Corradini, P. *Polym. Commun.* **1989**, *30*, 16.
(23) Venditto, V.; Guerra, G. M.; Corradini, P.; Fusco, R. *Polymer* **1990**, *31*, 530.
(24) Cavallo, L.; Guerra, G.; Vacatello, M.; Corradini, P. *Macromolecules* **1991**, *24*, 1784.
(25) Castonguay, L. A.; Rappé, A. K. *J. Am. Chem. Soc.* **1992**, *114*, 5832.
(26) Hart, J. R.; Rappé, A. K. *J. Am. Chem. Soc.* **1993**, *115*, 6159.
(27) Rappé, A. K.; Skiff, W. M.; Casewit, C. J. *Chem. Rev.* **2000**, *100*, 1435.
(28) Margl, P.; Deng, L.; Ziegler, T. *Organometallics* **1998**, *17*, 933.
(29) Ziegler, T.; Vanka, K.; Xu, Z. *C. R. Chim.* **2005**, *8*, 1552.
(30) Zurek, E.; Ziegler, T. *Faraday Discuss.* **2003**, *124*, 93.
(31) Vanka, K.; Chan, M. S. W.; Pye, C. C.; Ziegler, T. *Organometallics* **2000**, *19*, 1841.
(32) Chan, M. S. W.; Vanka, K.; Pye, C. C.; Ziegler, T. *Organometallics* **1999**, *18*, 4624.
(33) Xu, Z.; Vanka, K.; Firman, T.; Michalak, A.; Zurek, E.; Zhu, C.; Ziegler, T. *Organometallics* **2002**, *21*, 2444.
(34) Lanza, G.; Fragalà, I. L.; Marks, T. J. *J. Am. Chem. Soc.* **1998**, *120*, 8257.
(35) Lanza, G.; Fragalà, I. L.; Marks, T. J. *J. Am. Chem. Soc.* **2000**, *122*, 12764
(36) Lanza, G.; Fragalà, I. L.; Marks, T. J. *Organometallics* **2002**, *21*, 5594.
(37) Margl, P.; Deng, L.; Ziegler, T. *J. Am. Chem. Soc.* **1999**, *121*, 154
(38) Moscardi, G.; Resconi, L.; Cavallo, L. *Organometallics* **2001**, *20*, 1918.
(39) Yoshida, T.; Koga, N.; Morokuma, K. *Organometallics* **1996**, *15*, 766.
(40) Schaverien, C. J.; Ernst, R.; Terlouw, T.; Schut, P.; Sudmeijer, O.; Budzelaar, P. H. M. *J. Mol. Catal. A: Chem.* **1998**, *128*, 245.
(41) van der Leek, V.; Angermund, K.; Reffke, M.; Kleinschmidt, Goretzki, R.; Fink, G. *Chem. Eur. J.* **1997**, *3*, 585.
(42) Angermund, K.; Fink, G.; Jensen, V. R.; Kleinschmidt, R. *Macromol. Rapid Commun.* **2000**, *21*, 91.
(43) Graf, M.; Angermund, K.; Fink, G.; Thiel, W.; Jensen, V. R. *J. Organomet. Chem.* **2006**, *691* (21), 4367.
(44) te Velde, G.; Bickelhaupt, F. M.; van Gisbergen, S. J. A.; Fonseca Guerra, C.; Baerends, E. J.; Snijders, J. G.; Ziegler, T. *J. Comput. Chem.* **2001**, *22*, 931.
(45) Fonseca Guerra, C.; Snijders, J. G.; te Velde, G.; Baerends, E. J. *Theor. Chem. Acc.* **1998**, *99*, 391.
(46) ADF2004.01; SCM, Theoretical Chemistry, Vrije Universiteit, Amsterdam, The Netherlands (http://www.scm.com).
(47) Becke, A. D. *Phys. Rev. A* **1988**, *38*, 3098.
(48) Perdew, J. P. *Phys. Rev. B* **1986**, *33*, 8822.
(49) Perdew, J. P. *Phys. Rev. B* **1986**, *34*, 7406.
(50) Snijders, J. G.; Baerends, E. J.; Ros, P. *Mol. Phys.* **1979**, *38*, 1909.
(51) Boerrigter, P. M.; Baerends, E. J.; Snijders, J. G. *Chem. Phys.* **1988**, *122*, 357.
(52) Ziegler, T.; Tschinke, V.; Baerends, E. J.; Snijders, J. G.; Ravenek, W. *J. Phys. Chem.* **1989**, *93*, 3050.
(53) Tobisch, S. Unpublished results.
(54) Morokuma, K.; Maseras, F. *J. Comput. Chem.* **1995**, *117*, 5179.

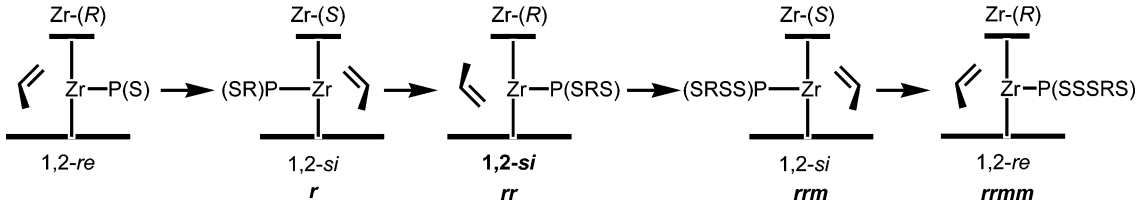

Figure 1. Schematic representation of the stereoerror sequence of enantiomeric misinsertion.

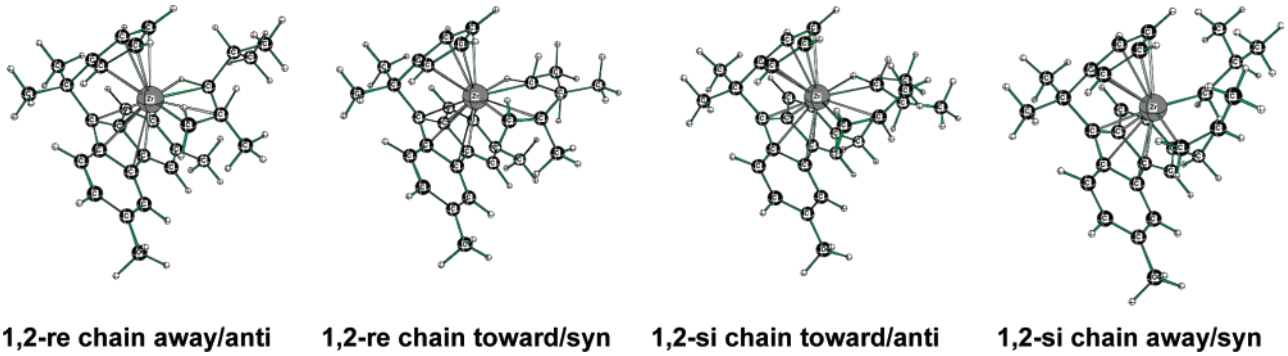

Figure 2. Gas-phase optimized transition states for the insertion of propylene into the Zr−C bond of **2a**.

Woo et al.[55] The part of the anion more closely in contact with the cation has been described at the QM level, while the bulky fluorinated side groups were described using modified SYBYL/TRIPOS 5.2 force field constants.[56] Cl atoms were used to cap the QM system, in order to mimic the electron-withdrawing effect of the perfluorinated arylic groups. A model for the anionic, methylated MAO was also studied, at the full QM level. The validity of such model in approximating the real, complex structure of MAO has been demonstrated in previous work from this group.[30−32] Solvent effects were estimated on the basis of gas-phase geometries with the conductor-like screening model (COSMO).[57,58] A dielectric constant of 2.38 was chosen, to represent toluene as the solvent. Only the electrostatic interaction with the solvent was computed. The radii used for the atoms (in Å) were as follows: C, 2.0; H, 1.16; B, 1.15; O, 1.5; F, 1.2; Zr, 2.4; Cl, 2.1; Si, 2.2; Al, 2.3. When the anion was included in the system, COSMO single-point calculations were carried out at the full-QM level on the gas-phase QM/MM optimized geometries.

All energies in the following discussion are given in kcal/mol relative to the parent reactants, as defined case by case in the text.

Results and Discussion

Enantioface Selectivity and Enantiotopic Site Control. There is unanimous consensus that the polymerization of α-olefins proceeds preferentially with 1,2-regiochemistry. Regioerrors deriving from 2,1-insertions can be as low as 1%, and the probability of consecutive regioerrors is virtually nil, also due to the fact that regioselectivity favoring 1,2-insertions is even more selective after a regioerror. In light of this finding, the possibility of different regioselectivity has not been considered in this work. It has been further assumed that all insertions proceed in a 1,2-fashion.

Many research groups have shown that there are mainly two factors determining the olefin enantioface exposed during the insertion. First, the olefin side group and the alkyl chain representing the growing polymer tend to be as far apart as possible, to reduce steric repulsion. This means that a mutual anti arrangement is preferable to a syn one. Second, for the same reason the alkyl chain tends to maximize the distance from the ligands, in particular the one which is larger.

In the case of C_s-symmetric systems derived from the complexes first introduced by Ewen and Razavi,[3] the polymer chain tends to stay away from the fluorenyl ligand. The preferred enchainment sequence and an enantiomeric misinsertion event can therefore be depicted schematically as in Figure 1.

The chirality of the metal center is assigned using the Cahn−Ingold−Prelog rules, as extended to chiral metallocenes by Stanley and Baird[59] and Schlögl.[60] Each step represents a full catalytic cycle from the depicted π complex to that obtained after insertion, followed by uptake of the next monomer unit (the π complex is not necessarily the resting state; it has been chosen only to explain the stereochemistry). At each step, the polymer chain is assumed to be oriented away from the bulky Flu ligand. In the preferred stereochemical sequence, the methyl group of propylene and the polymer chain are in an anti stereochemical relationship (from now on, this conformation will be called chain-away/anti) and one of the two faces of propylene, termed re or si,[61] is inserted preferentially. Propylene π complexes in which Zr has an *S* configuration insert the monomer in a 1,2-si fashion, and the configuration of the chiral center on the alkyl chain, which is closest to the metal center, is *R*. When the configuration of Zr is *R*, the closest chiral center on the chain is of the *S* kind and a 1,2-re insertion occurs. At each insertion the alkyl chain "swings" from one coordination site to the other (as represented more in detail in the section on site epimerization), which ensures alternating chiral centers along the polymer chain, as required in a syndiotactic polymer. Due to the enantiotopic nature of the metallic center, to have a complete picture it is necessary to study only one of the two possibilities. Therefore, in all the π complexes and transition states discussed in this work the Zr center has an *R* configuration.

(55) Woo, T. K.; Cavallo, L.; Ziegler, T. *Theor. Chem. Acc.* **1998**, *100*, 307.
(56) Clark, M.; Cramer, R. D. I.; van Opdenbosch, N. *J. Comput. Chem.* **1989**, *10*, 982.
(57) Klamt, A.; Schuurmann, G. *J. Chem. Soc., Perkin Trans.* 2 **1993**, 982.
(58) Pye, C. C.; Ziegler, T. *Theor. Chem. Acc.* **1999**, *101*, 396.
(59) Stanley, K.; Baird, M. C. *J. Am. Chem. Soc.* **1975**, *97*, 6598.
(60) Schlögl, K. *Top. Stereochem.* **1966**, *1*, 39.
(61) Hanson, K. R. *J. Am. Chem. Soc.* **1966**, *88*, 2731.

Table 1. Gas-Phase Energies of Propylene π Complexes and Corresponding Insertion Transition States for Different Ligand Systems[a]

	π complex		TS_{INS}	
species	1,2-re	1,2-si	1,2-re	1,2-si
2a	−11.9/−9.3 (ch-aw/anti)	−7.6/−1.3 (ch-tow/anti)	−6.7/−7.4 (ch-aw/anti)	−5.0/−4.0 (ch-tow/anti)
	−6.4/−0.6 (ch-tow/syn)	−12.3/−9.0 (ch-aw/syn)	−2.8/0.9 (ch-tow/syn)	−4.5/−4.5 (ch-aw/syn)
2b	−9.9/−6.6 (ch-aw/anti)	−4.7 (ch-tow/anti)	−5.6/−5.6 (ch-aw/anti)	−3.4/−1.3 (ch-tow/anti)
	−3.4/2.9 (ch-tow/syn)	−10.1/−6.3 (ch-aw/syn)	−0.1/− (ch-tow/syn)	−3.7/−3.1 (ch-aw/syn)
3			−4.7/−5.0 (ch-tow/anti)	−1.9/−1.6 (ch-aw/anti)
				−2.4/−2.0 (ch-aw/syn)

[a] All energies are relative to the parent iBu alkyl complex precursor and propylene. Relative energies are given in kcal/mol.

Table 2. Energies of Propylene π Complexes and Corresponding Insertion Transition States for Different Ligand Systems, in Toluene[a]

	π complex		TS_{INS}	
species	1,2-re	1,2-si	1,2-re	1,2-si
2a	−11.2/−8.6 (ch-aw/anti)	−6.8/−0.7 (ch-tow/anti)	−5.6/−6.5 (ch-aw/anti)	−4.0/−2.9 (ch-tow/anti)
	−6.0/−0.2 (ch-tow/syn)	−11.8/−8.4 (ch-aw/syn)	−1.8/1.9 (ch-tow/syn)	−3.3/−3.5 (ch-aw/syn)
2b	−9.5/−6.1 (ch-aw/anti)	−4.3/−(ch-tow/anti)	−4.7/−4.6 (ch-aw/anti)	−2.6/− (ch-tow/anti)
	−3.4/3.0 (ch-tow/syn)	−9.7/−5.9 (ch-aw/syn)	−0.0/− (ch-tow/syn)	−2.9/−2.3 (ch-aw/syn)
3			−5.5/−5.8 (ch-tow/anti)	−2.7/−2.4 (ch-aw/anti)
				−3.0/−3.0 (ch-aw/syn)

[a] All energies are relative to the parent iBu alkyl complex rrecursor and propylene. Relative energies are given in kcal/mol.

1,2-si enantiomeric misinsertions occur when either the polymer chain points away from the Flu group and the olefin substituent is syn to it (conformation "chain-away/syn") or when it points toward the Flu group, while maintaining an anti relationship with the olefin substituent ("chain-toward/anti"). The situation in which the polymer chain points toward the Flu ligand and is in a syn relationship with the methyl group of propylene ("chain-toward/syn") would lead to 1,2-re insertion with the "correct" enantioface, but it is expected to be the highest in energy.

The energies of the π complexes and of the resulting insertion TS's have been computed for all the four conformations mentioned above (ch-aw/anti, ch-tow/anti, ch-tow/syn, and ch-aw/syn in Table 1), with catalysts **1**−**3**, whose structures are shown in Chart 1.

Ewen's and Razavi's basic system **1** has been studied by Angermund et al., using a combination of DFT functional and basis set very similar to that chosen by us.[42] We have extensively studied the substituted system **2a**, bearing Me groups in the 3- and 6-positions of the Flu moiety. An i-Bu group has been chosen as the shortest alkyl chain capable of representing well enough the growing polymer. **2b**, having a bridging Si atom instead of a carbon atom, has also been considered. Furthermore, the transition states for the 1,2 insertion have been optimized also for **3**, the carbon-bridged system bearing two t-Bu groups in the 3,6 positions of the fluorenyl ligand. In Table 1 are reported the energies of the gas-phase optimized structures, relative to the respective parent zirconocene-alkyl cationic complexes plus propylene.

In all cases, at least one rotamer of the i-Bu group has been optimized for each conformation. The optimized insertion transition state geometries of **2a** in the most stable rotamer of each conformation are displayed in Figure 2. As expected, for all ligand systems the lowest conformation is the one in which the alkyl chain points away from the Flu moiety ("ch-aw") and the spatial relationship between it and the Me group of propylene is anti. This corresponds to a 1,2-re approach (since the *R* chirality has been chosen for the metallic center). The 1,2-si insertions are slightly less favorable, because one of the two interactions (either alkyl chain−monomer or alkyl chain−catalyst) is not minimized. When both interactions are unfavorable, there is a dramatic increase in the relative energy. The remaining channel following a 1,2-re approach is therefore considerably higher in energy than all the others.

The stability trend is the same for the π complexes and the transition states, in agreement with previous computational research.[22] Using π complexes for determining stereoselectivity can lead to qualitatively correct conclusions; however, for more accurate predictions it is obviously necessary to use data from TS optimizations. It is worth noting that if the anion is not included, formation of the π complex is generally exothermic (0.6−11.9 kcal/mol for **2a** and −10.1 to +2.9 kcal/mol for **2b**). It certainly would be physically more realistic to include the anion. In that case the monomer uptake would be raised in energy by almost 20 kcal/mol (such is the strength of the cation−anion interaction; see the section on site epimerization), because of the energy penalty paid to abstract the anion and free a coordination site of the cation. However, although clearly absolute reaction rates cannot be computed without considering the anion, it is true that the anion does not play an important role in stabilizing a conformation of the cation rather than another one. Therefore, enantioface selectivity is hardly affected and the anion can be disregarded in this series of calculations.

The substitution pattern on the Flu ligand, instead, plays an important role in the stereoselectivity.

Adding bulky groups to the 3,6-positions strengthens repulsive interactions and increases the energy gap between the four conformations, as can be seen in the **1**−**2a**−**3** sequence: the selectivity for **1** is 2.0 kcal/mol,[43] for **2a** it is 2.4 kcal/mol, and for **3** it is 2.6 kcal/mol. Because of its bulk, the t-Bu substituent exerts the greatest conformational constraints on the growing polymer chain and consequently exhibits the highest enantiofacial selectivity. The increased selectivity comes only at a marginal expense of reactivity. In fact, in the gas phase the energy of the most favorable TS for the **2a** substituted system (**TS2a aw/anti**) is 7.4 kcal/mol below the reference energy point (zirconocenium i-Bu complex + propylene), whereas that of the most favorable TS for **3** (**TS3 aw/anti**) is 5.0 kcal below the reference energy point. It should be added that when the counterion is taken into account, both transition states would be destabilized because in the reference state the anion and

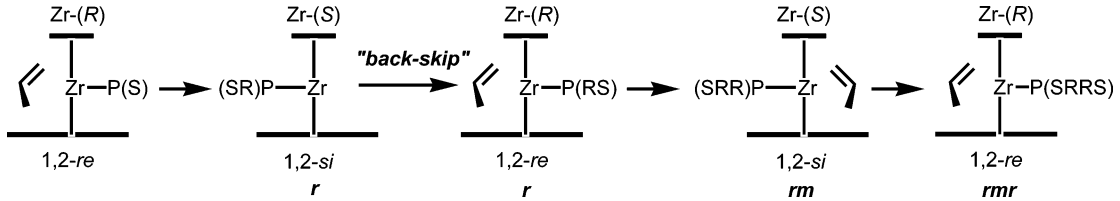

Figure 3. Schematic representation of the stereochemical sequence leading to the generation of stereoerrors due to site epimerization.

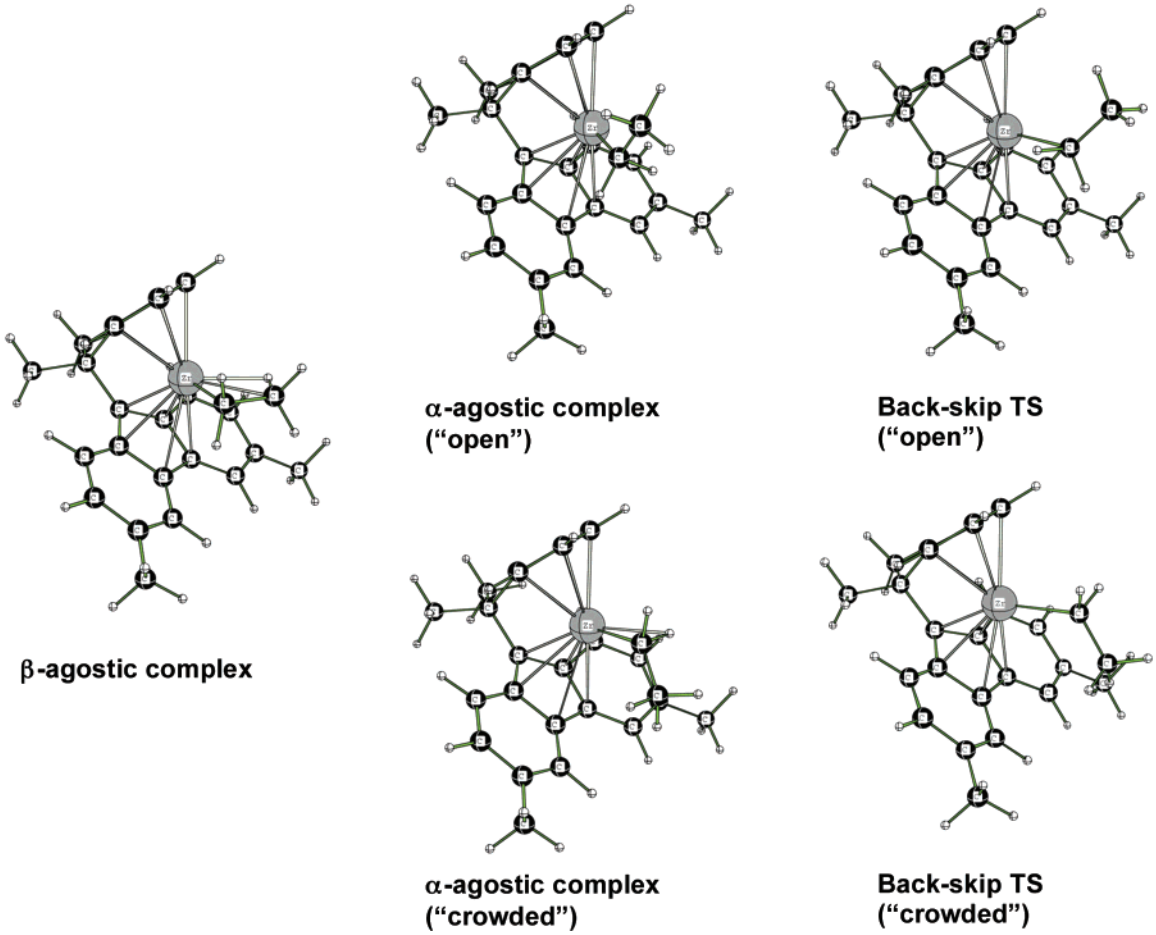

Figure 4. Local minima and transition states encountered during the site epimerization mechanism involving **2a** without assistance from the anion.

cation interact closely. Due to the different bulks of the substituents, it is likely that the ion-pair energy is weaker in **3**.

If this is true, then the difference in reactivity of the two systems would be even smaller; if the difference in the ion-pairing energy is large enough, **3** could even be the most reactive species. As already observed experimentally, the presence of a Si bridge is detrimental for enantioface selectivity (selectivity of 2.4 kcal/mol for **2a**, as opposed to 1.8 kcal/mol for **2b**).

The influence of toluene solvation on **2a**, **2b**, and **3** has been estimated by calculating the solvation energies of the gas-phase optimized geometries. The relative energies of the species involved in the insertion process are reported in Table 2. Unsurprisingly, for all the different ligand systems, solvation effects are comparable for the four competing channels. $\Delta\Delta E$'s range between 0.1 and 0.2 kcal/mol: differential solvation plays a minimal role.

Site Epimerization. Site epimerization occurs when, after the insertion, the alkyl chain moves to the empty coordination site of the metal. The rate of the process does not depend on monomer concentration, whereas normal propagation does. Therefore, the frequency of site epimerization increases when the propagation slows down: for example, when most of the monomer has been consumed.

The preferred enchainment sequence and an intervening site epimerization event are depicted schematically in Figure 3.

Two mechanisms can be conceived for the site epimerization, one of which does not require taking the anion into account. The movement required to bring the alkyl chain to the other vacant coordination site of the metal involves the transformation of the β-agostic resting state into a symmetrical β'-agostic one, via a transition state in which the alkyl chain rests approximately on the plane formed by the metal and the ligands' centroids. During the transformation, on either side or the reaction energy profile there is an intermediate α- and α′-agostic complex. Such a mechanism has been modeled recently also by other groups.[19,43] The alkyl chain can rotate in two directions, which are not equivalent if the ligands are not the same. In the case of **2a** and **2b**, the rotation is easier from the less hindered side, that of the Cp ligand. Figure 4 depicts the intermediate structures and the transition states for the site epimerization of **2a**, in the case where the alkyl chain is an ethyl group. A larger number of intermediate structures, linked to each other by conformational

Table 3. Relative Energies of Local Minima and Transition States Involved in the Site Epimerization of Naked Alkyl Zirconocene Cations[a]

species	2a	2b	bis-Cp[b] (CH_2 bridge)
Et-β	0	0	0[c]
Et-α crowd	9.7	9.4	
Et-α open	7.0	8.6	8.9[c]
Et-TS crowd	12.6	12.0	
Et-TS open	12.5	11.5	10.3[c]
iBu-β	0		0
iBu-γ1 crowd	3.2		1.8
iBu-γ2 crowd	1.6		
iBu-α1 crowd	13.8		
iBu-α2 crowd	10.6		
iBu-α3 crowd	13.4		
iBu-α1 open	8.8		11.5
iBu-α2 open	8.8		9.6
iBu-α3 open	10.8		11.4
iBu-TS1 open	13.1		12.4

[a] Energies are given in kcal/mol, relative to the most stable conformer. [b] From ref 43. [c] Propyl complex.

equilibria, can exist for more complex alkyl groups such as the isobutyl group. Graf et al. have studied these conformational equilibria in detail for a simple CH_2-bridged bis(cyclopentadienyl) zirconocene.[43] In the top series of structures the alkyl group rotates from the side of the less bulky Cp ligand ("open" rotation). In the bottom series of structures the rotation is more hindered by the bulkier Flu ligand ("crowded" rotation).

On the less hindered side, the rotation is only marginally affected by the presence of the distant large fluorenyl ligand, as can be seen by comparing our results with those obtained by Graf et al. in ref 43 (see Table 3).

The barrier depends somewhat on the size of the rotating alkyl chain: as expected, an ethyl group is slowed down less than a larger isobutyl group (which is the actual product from the first insertion and simulates better the growing polymer chain). Overall, the activation energy of the site epimerization mechanism that does not take into account the counteranion is quite large, likely too much to fit the experimental results, which show that the pentad distribution is indeed influenced by site epimerization. If this rather slow process is coupled with a virtually barrierless, highly exothermic process like the anion reassociation, it is likely that a much lower activation energy is found. It is therefore expected that a much more viable mechanism exists, in which the counterion assists the site epimerization.

In the regular polymerization process, the anion is displaced when a monomer unit is taken up by the cation. Assuming monomer uptake occurred along the most favorable route, i.e., cis to the anion, right after the insertion, the anion is in an outer coordination sphere, on the side of the alkyl chain (see Chart 1). In the model used for this study, the alkyl chain is composed of seven carbons, as resulting from two consecutive 1,2-propylene insertions. The cation has an empty coordination site, available for the formation of a close contact ion pair. The anion can first undergo a spatial reorganization in the outer coordination sphere, then approaching unhindered the free coordination site, or it can approach the cation directly, in the process pushing the alkyl chain to the other coordination site.

The first process is what normally occurs during propagation, while the second corresponds to the site epimerization. In fact, the immediate ion pairing and the simultaneous displacement of the alkyl chain result in a complex in which the alkyl chain occupies the same coordination step as in the previous catalytic cycle.

It can be reasonably assumed that the anion reorganization in the outer coordination sphere occurs freely and that it is

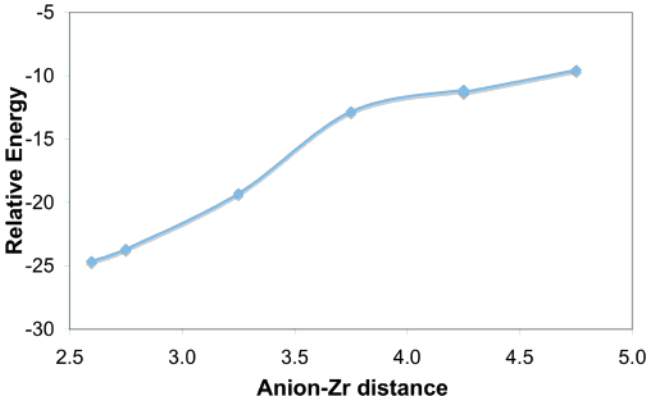

Figure 5. Ion pairing in the regular polymerization mechanism involving **2a**, after the diffusion-controlled anion reorganization. Distances are in Å and energies in kcal/mol.

Table 4. Dependence of the Relative Energies of the Species Involved in the Site Epimerization on the Nature of the Ligand System[a]

	gas phase			sol (toluene)		
	β-agostic product	TS_{SE}	ion pair[b]	β-agostic product	TS_{SE}	ion pair[b]
1	−5.3	−2.0	−23.9	−9.9	−5.9	−25.6
2a	−4.3	−1.7	−23.0	−9.9	−6.5	−25.5
2b	−6.6	−4.1	−23.2	−12.8	−9.9	−25.9
3	−5.9	−0.6	−22.9	−11.3	−4.8	−20.9

[a] The counteranion is $MeB(C_6F_5)_3^-$. All energies are relative to the respective parent close-contact ion-pair precursor and propylene. Relative energies are given in kcal/mol. [b] With the chosen reference state, this value corresponds to $\Delta E_{reaction}$.

Table 5. Dependence of the Relative Energies of the Species Involved in the Site Epimerization on the Nature of the Counteranion[a]

	gas phase			sol (toluene)		
	β-agostic product	TS_{SE}	ion pair[b]	β-agostic product	TS_{SE}	ion pair[b]
$MeB(C_6F_5)_3^-$	−4.3	−1.7	−23.0	−9.9	−6.5	−25.5
$MAOMe^-$	5.2	6.3	−25.8	−3.4	0.4	−25.7
$FAl(Bip_f)_3^-$	6.1	8.2	−24.1	2.3	6.7	−25.4

[a] The ligand system is **2a**. All energies are relative to the respective parent close-contact ion-pair precursor and propylene. Relative energies are given in kcal/mol. [b] With the chosen reference state, this value corresponds to $\Delta E_{reaction}$.

governed by diffusion. Indeed, gas-phase calculations show that for our standard system, **2a-MeB(C_6F_5)$_3$**, the barrier is 0.5 kcal/mol, within the error associated with the computational method. Formation of the close-contact ion pair is then exothermic and spontaneous on the potential energy surface, as can be seen from the reaction coordinate shown in Figure 5, which depicts the reassociation of the $MeB(C_6F_5)_3^-$ anion with the cation. The exothermicity of the ion pairing is such (∼20 kcal/mol) that the process is irreversible. Incidentally, when the anion is included in the description, the monomer uptake is possible, albeit endothermic, only because the energetically expensive rupture of the ion pair occurs at the same time the weaker interaction of the π-complex is formed. The resting state is therefore the ion pair. The reaction is driven by the insertion step, which makes the overall catalytic cycle exothermic by around 25 kcal/mol (as shown in Tables 4 and 5).

The ion pairing without previous anion reorganization instead has an activation barrier, due to the fact that the metal−alkyl interaction must be weakened, while repulsive interactions increase as the anion pushes the alkyl chain to the other

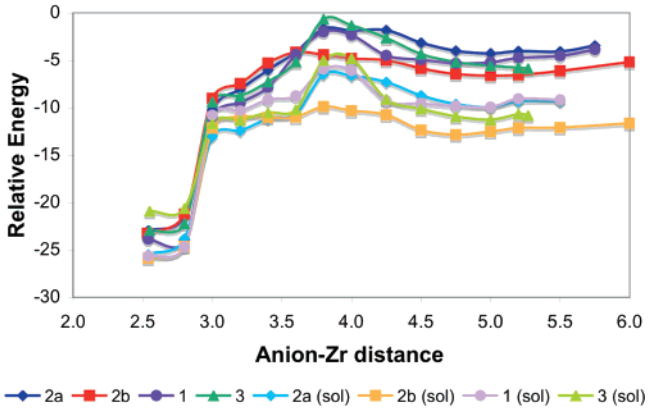

Figure 6. Site epimerization reaction coordinates for systems **1**, **2a**, **2b**, and **3**, in the gas phase and in toluene. Energies are relative to the respective parent L_2Zr-iBu$^+$MeB$(C_6F_5)_3^-$ ion pairs plus propylene.

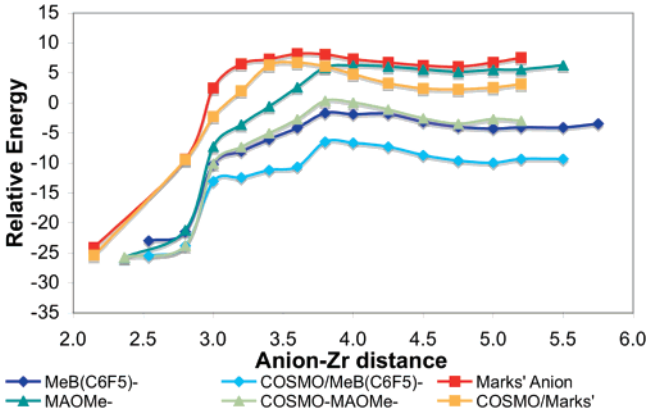

Figure 7. Influence of the counteranion on the site epimerization reaction profile in the gas phase and in toluene solution. The anions studied are MeB$(C_6F_5)_3^-$, AlF$(Bif_f)_3^-$, and a model for MAO-Me$^-$. In all cases the cation is **2a**. Energies are relative to the respective parent **2a-X** ion pairs plus propylene.

coordination site. All along the site epimerization, the β-agostic interaction is maintained. Only past the transition state is the agostic interaction lost, at a point where the energetic cost of its loss is overshadowed by the gain from the ion pairing. The reaction coordinates for the anion-assisted site epimerization are shown in Figure 6 for systems **1**, **2a**, **2b**, and **3**, both in the gas phase and in toluene solution.

The extent of the barrier depends on the charge distribution of the anion and on the ligand system. The computed barriers to the site epimerization with the aforementioned set of ligands, in the gas phase and in toluene solution, are given in Table 4. The counterion used for all these calculations was MeB$(C_6F_5)_3^-$, as in the calculations on the ion pairing in the regular mechanism. The effect of the substituents in the 3,6-positions of the fluorenyl ligand is not linear. The site epimerization actually seems to increase from **1** (barrier of 3.3 kcal/mol) to **2a** (barrier of 2.6 kcal/mol). When the substituents are large enough, as in **3**, repulsive steric interactions are increased and the barrier to site epimerization reaches its maximum (5.3 kcal/mol in the gas phase). Substituting the bridging carbon atom with that of silicon (**2b**) increases the occurrence of site epimerization (barrier of 2.5 kcal/mol). This is in agreement with the experimental results obtained by Waymouth et al.[62,63] The effect is more evident when the interaction with the solvent is included: the barrier for **2a** in solution is 3.4 kcal/mol, whereas for **2b** it is only 2.9 kcal/mol (see Table 4).

As can be seen from Table 4 and Figure 6, for all the systems, in general the effect of solvation is to stabilize the species involved, relative to the reactants: that is, the L_2Zr-iBu$^+$MeB$(C_6F_5)_3^-$ close-contact ion pair plus propylene.

The extent of the stabilization, however, is not the same as the site epimerization proceeds, and is also dependent on the nature of the ligand system. Differential solvation of the species along the reaction coordinate is due to the shifting charge distribution. The solvation model used computes the electrostatic interaction between the solute and the polarizable continuum representing the solvent. A charged solute interacts more with the solvent than a neutral solute. Likewise, a loose ion pair interacts more with the solvent than a tight ion pair. The SE transition state is a tighter ion pair than the β-agostic addition product; thus, it is less stabilized by the solvent. As the reactant is stabilized with respect to the transition state, the activation energy for the site epimerization is higher in solution than in the gas phase. The trend observed in the gas phase, however, is maintained qualitatively: **1** has a higher barrier than **2a**, while **3** still is the most efficient system at suppressing site epimerization.

As further evidence of the importance of charge distribution in the differential solvation of the species involved, the site epimerization of **2a** in the presence of three different anions was investigated. In addition to the already mentioned MeB$(C_6F_5)_3^-$, the site epimerization was studied with Marks' fluoroaluminate, FAl$(Bif_f)_3$,[64−66] and with a model representing methylated MAO.[30] The reaction profiles, in the gas phase and in toluene, are shown in Figure 7. The energies of the species are reported in Table 5. Marks' anion is much bulkier than MeB$(C_6F_5)_3^-$, while its negative charge is more concentrated on the fluorine, which bridges with the zirconocenium cation. The model for the methylated MAO also has the negative charge more concentrated in the part that interacts with the cation, compared to the case for MeB$(C_6F_5)_3^-$, while the steric bulk is lower than that of FAl$(Bif_f)_3^-$ and comparable to that of MeB$(C_6F_5)_3^-$.

The results obtained from gas-phase calculations suggest that site epimerization should occur most easily with MAO (ΔE = 1.1 kcal/mol) and then with Marks' anion (ΔE = 2.1 kcal/mol), while MeB$(C_6F_5)_3^-$ should be the best anion for reducing site epimerization to a minimum (ΔE = 2.6 kcal/mol). This does not match the experimental results published by Marks et al. However, if solvation is considered, the correct qualitative trend is obtained: Marks' anion is still the most effective in reducing the site epimerization (ΔE = 4.4 kcal/mol), with the likelihood of site epimerization increasing when MAO or MeB$(C_6F_5)_3^-$ is used to activate the Zr−Me bond of the precatalyst (ΔE = 3.8 and 3.4 kcal/mol, respectively). The reason is twofold. First, Marks' anion interacts more strongly with the solvent than do the other anions, because its charge is the most localized. Therefore, solvent destabilization of the TS with respect to the reactant is highest for Marks' anion. Second, the steric bulk makes it more difficult for the fluoroaluminate to get close to the zirconocenium cation. The MAO-Me$^-$ model also has a more concentrated charge than MeB$(C_6F_5)_3^-$, which in solution

(62) Fan, W.; Leclerc, M. K.; Waymouth, R. M. *J. Am. Chem. Soc.* **2001**, *123*, 9555.
(63) Gomez, F. J.; Waymouth, R. M. *Macromolecules* **2002**, *35*, 3358.
(64) Chen, Y.-X.; Metz, M. V.; Li, L.; Stern, C. L.; Marks, T. J. *J. Am. Chem. Soc.* **1998**, *120*, 6287.
(65) Chen, M.-C.; Marks, T. J. *J. Am. Chem. Soc.* **2001**, *123*, 11803.
(66) Chen, M.-C.; Roberts, J. A. S.; Marks, T. J. *J. Am. Chem. Soc.* **2004**, *126*, 4605.

Scheme 2. Anion Dynamics in the Normal Propagation Process and in the Site Epimerization

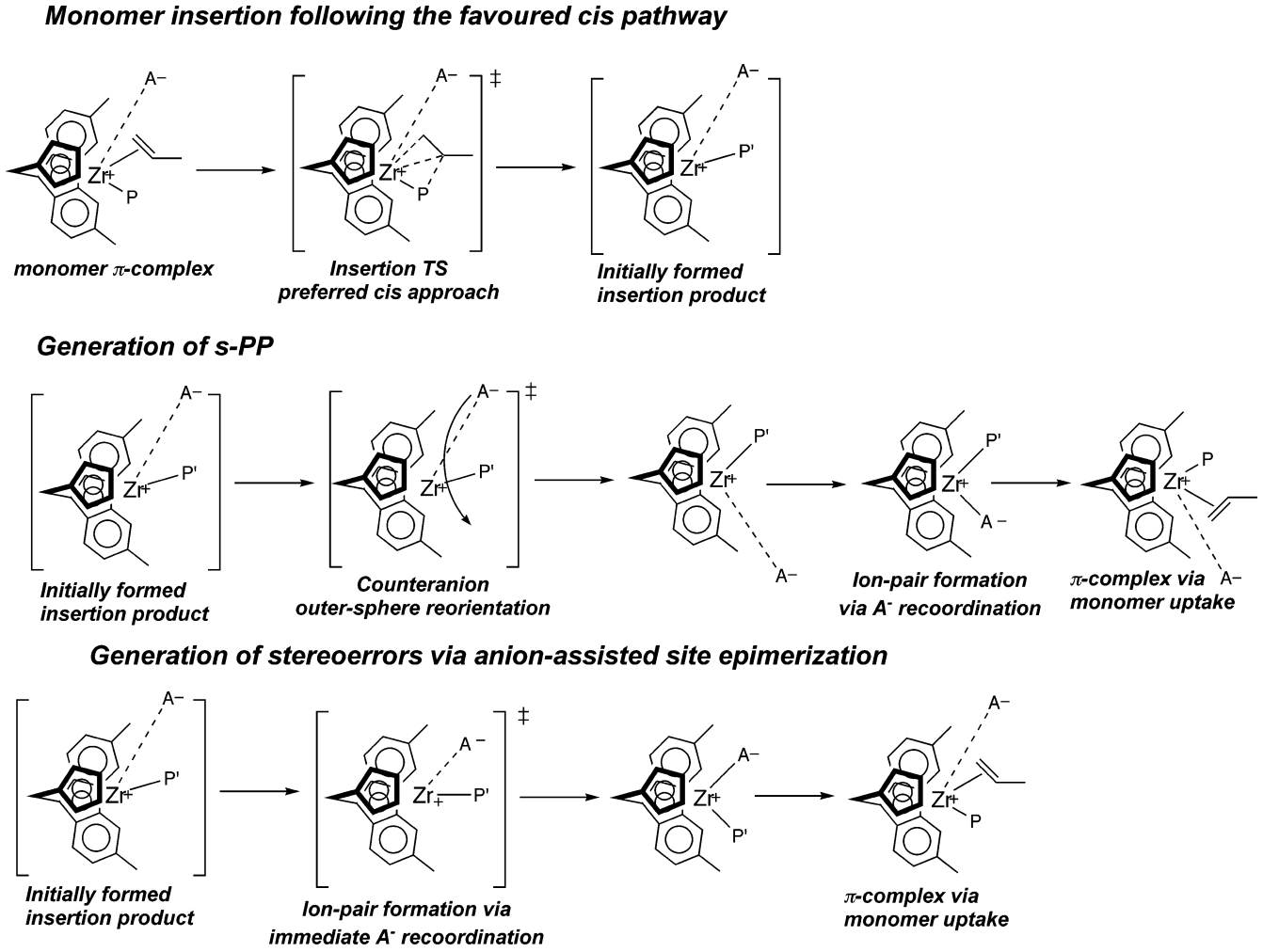

has an effect similar to that found for Marks' anion. At the same time, it is smaller than Marks' anion; therefore, sterics do not contribute as much to the barrier. The two effects combined are capable of explaining the experimental results.

Computational Prediction of the Pentad Distribution. In a perfect syndiotactic polymerization, insertions always have 1,2-regioselectivity, no misinsertion or site epimerization events occur and all dyads are of the *r* kind. Starting from the resting state (the ion pair), first a monomer unit is taken up in a slightly endothermic process and then inserted into the Zr−C bond. The latter step is exothermic and irreversible; its product is a new Zr−alkyl complex with the anion in the outer coordination shell. The anion reassociation, which regenerates the ion-pair resting state, is also irreversible, as previously shown, and can proceed in two ways, one of which is the site epimerization. Since the two events (insertion and ion pairing) are irreversible, they are independent of each other. It is therefore possible to identify all the combinations of events in a single catalytic cycle and assign them probabilities, as products of the probabilities of individual events. For stereorigid catalysts with a well-defined stereochemical site control, it is straightforward to predict qualitatively the polymer microstructure, on the basis of symmetry considerations. A number of relatively simple statistical methods have also been developed, which allow predicting the microstructure with almost quantitative accuracy.[67−70]

According to the model presented in Scheme 2, every catalytic cycle has four possible stereochemical outcomes. The model assumes that all insertions occur with 1,2-regioselectivity and that ion pairing is irreversible; it admits the possibility of a defective alternating mechanism (possibility of SE) and assumes that the catalytic site is responsible for the control of stereochemistry (i.e., there is no chain end control). All these assumptions are quite reasonable and are based on previous experimental and theoretical evidence, as well as on results shown in previous sections of this paper. Further discussion on the importance of chain end control will be presented in the last section.

The probability parameters reported in Scheme 3 have been named as in the work by Farina et al.[11] Parameter **a** is defined as the probability that the entering monomer unit assumes a certain configuration at a given catalytic site. Parameter **c** is defined as the probability that two successive additions occur at the same site related to parameter **a**. Since the system is C_s symmetric, the probability of a site epimerization event is independent of which coordination site is taken by the alkyl chain; the same holds for the probability of a misinsertion (i.e.,

(67) Angermund, K.; Fink, G.; Jensen, V. R.; Kleinschmidt, R. *Chem. Rev.* **2000**, *100*, 1457.

(68) Herfert, N.; Fink, G. *Makromol. Chem. Macromol. Symp.* **1993**, *66*, 157.

(69) Farina, M.; Di Silvestro, G.; Sozzani, P. *Macromolecules* **1993**, *26*, 946.

(70) Farina, M.; Di Silvestro, G.; Terragni, A. *Macromol. Chem. Phys.* **1995**, *196*, 353.

Scheme 3. Possible Stereochemical Outcomes Following a Catalytic Cycle and Associated Probabilities

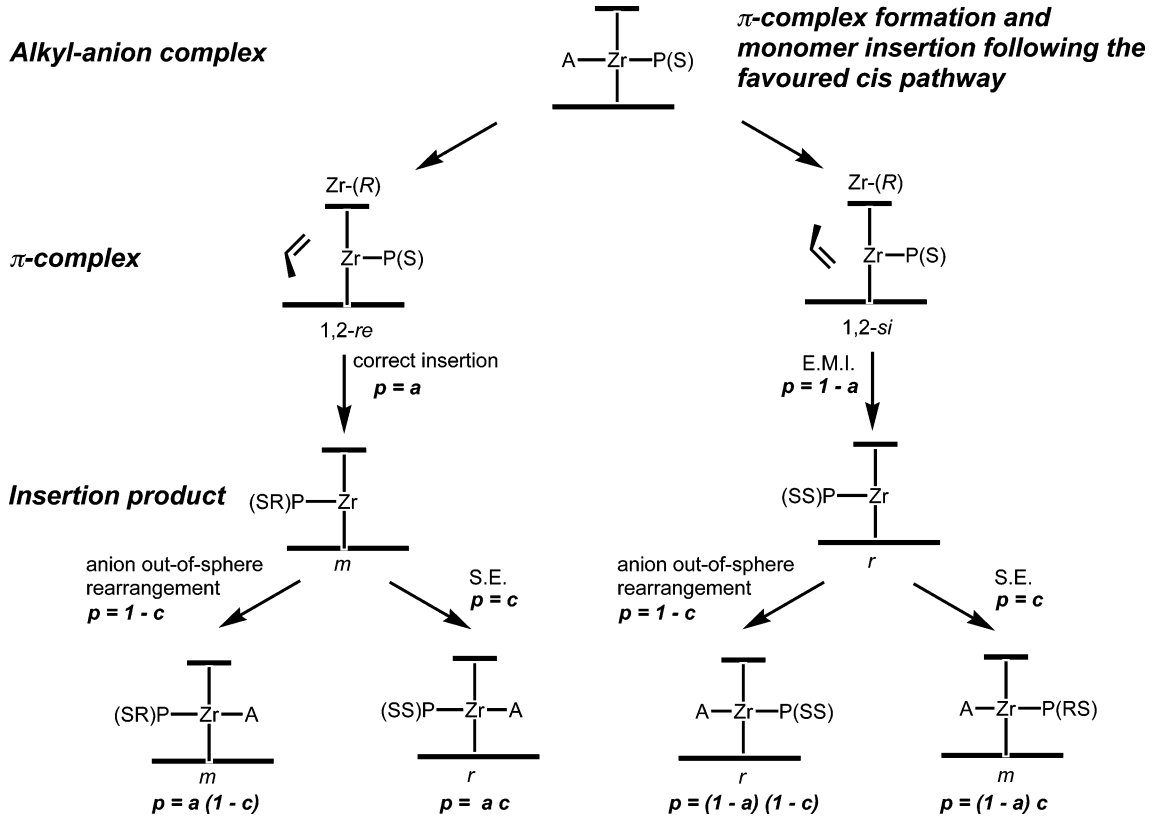

for the other catalytic site, parameters b and d can be defined in the same way as a and c, so that $1 - a = b$ and $c = d$).

By repeating the cycle five times, it is possible to obtain all possible stereochemical outcomes in the generation of a pentad, which are $4^5 = 1024$. Each of the 1024 outcomes has a probability which is a polynomial in a and c. Every pentad can be produced by more than one unique sequence of events; the overall weight of a pentad in the distribution depends on how likely are the unique sequences of events that contribute to it. The expressions for each pentad are complex summations of polynomials and have been determined by Farina and coworkers.[11,69,70]

For example, below are reported the probabilities for the *rrrm* and *rrrr* pentads ($e = 1 - a$ and $g = 1 - c$):

$$[rrrm] = 2ae(ac + eg)(ag + ec)[(a^2(ag^2 + ec^2) + e^2(ac^2 + eg^2)] + 2aecg[(ac + eg)^2 + (ag + ec)^2 \quad (1)$$

$$[rrrr] = a^2(ag + ec)^2(ag^2 + ec^2) + e^2(ac + eg)^2(ac^2 + eg^2) + 2aecg(ac + eg)(ag + ec) \quad (2)$$

It is therefore possible to compute a pentad distribution only from data on enantioface selectivity and site epimerization. Theoretical pentad distributions for the systems studied are reported for different temperatures in Table 6. As expected, **3** produces s-PP with the highest content of *rrrr* syndiotactic pentads, the effect of combined higher enantioface selectivity and reduced site epimerization. For **3** the 6.5 kcal/mol value for $\Delta\Delta E_{SE}$ is so high that site epimerization is essentially nonexistent, as can be seen from the absence of a signal for the combined [*mrmm*] + [*rmrr*] pentads. The agreement between the theoretically predicted and the experimental pentad distributions, obtained under various conditions (see Table 7), is good, particularly at low temperatures. It is likely that the poorer agreement at higher temperatures is due to entropic factors, which are not accounted for in the calculations, and possibly to other chemical processes, such as the back-side attack or, less likely, the chain epimerization.

As already mentioned by Marks,[18] *m* stereoerrors can in principle also be generated through the correct stereochemistry of propylene insertion from a π complex obtained via the back-side attack of propylene to the alkyl complex, i.e., trans uptake with respect to the anion, instead of the preferred cis uptake. The result of the back-side attack is the same as that of the site epimerization, in that it forces the alkyl chain to change coordination site. Although the results of the two events are indistinguishable, they take place in different parts of the catalytic cycle; thus, if the back-side attack is a viable option, its influence should be incorporated in term c, which would then reflect the contributions of two independent events.[18]

Therefore, the cis and trans coordination (back-side attack) of propylene to the i-Bu alkyl complex of system **2a** has been

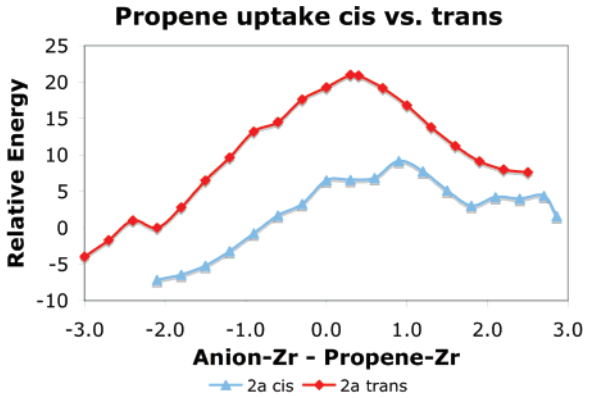

Figure 8. Gas-phase energy profile for the cis and trans uptake of propylene to yield π complex **2a**, in the presence of $MeB(C_6F_5)_3^-$ as the counteranion.

Table 6. Predicted Pentad Distributions, Based on the Selectivities for Site Epimerization and Enantioface Misinsertion Computed in Toluene Solution, Using $MeB(C_6F_5)_3^-$ as the Anion

temp, °C	[*mmmm*]	[*mmmr*]	[*rmmr*]	[*mmrr*]	[*mrmm*] + [*rrmr*]	[*mrmr*]	[*rrrr*]	[*rrrm*]	[*mrrm*]
Computed Pentad Distributions (%) of PP Generated by **1**[a,e]									
10	0	0	2	5	0	0	87	5	0
50	0	0	4	7	1	0	80	7	0
70	0	1	4	8	1	0	76	9	0
100	0	1	5	10	2	0	71	10	0
Computed Pentad Distributions (%) of PP Generated by **2a**[b,e]									
10	0	0	1	2	1	0	93	3	0
50	0	0	2	4	1	0	89	5	0
70	0	0	2	4	1	0	86	6	0
100	0	0	3	6	2	0	81	7	0
Computed Pentad Distributions (%) of PP Generated by **2b**[c,e]									
10	0	0	3	7	2	0	80	7	0
50	0	1	4	9	3	0	71	10	0
70	0	1	5	10	4	0	67	12	1
100	1	1	5	11	5	0	61	13	1
Computed Pentad Distributions (%) of PP Generated by **3**[d,e]									
10	0	0	1	1	0	0	97	1	0
50	0	0	1	2	0	0	94	2	0
70	0	0	2	3	0	0	92	3	0
100	0	0	2	3	0	0	89	4	0

[a] $\Delta\Delta E_{EMI} = 2.0$ kcal/mol, $\Delta\Delta E_{SE} = 4.0$ kcal/mol. [b] $\Delta\Delta E_{EMI} = 2.5$ kcal/mol, $\Delta\Delta E_{SE} = 3.4$ kcal/mol. [c] $\Delta\Delta E_{EMI} = 1.8$ kcal/mol, $\Delta\Delta E_{SE} = 2.9$ kcal/mol. [d] $\Delta\Delta E_{EMI} = 2.8$ kcal/mol, $\Delta\Delta E_{SE} = 6.5$ kcal/mol. [e] $\Delta\Delta E_{EMI}$ = energy difference between insertion with the "right" enantioface and "wrong" enantioface. $\Delta\Delta E_{SE}$ = energy difference between normal anion reassociation and anion-assisted site epimerization (see text for more details).

Table 7. Experimentally Determined Pentad Distributions in the Polymerization of Propylene with 1 and Its Si Bridge Variant 1b, under a Variety of Experimental Conditions[a]

item	*P* (bar)	solvent	*T* (°C)	*a*	*c*	$\Delta\Delta G^{\ddagger}$ EMI	$\Delta\Delta G^{\ddagger}$ SE	cat. syst	stoich[b]
1	1.3	toluene	−30	0.987	0.005	2.09	2.56	**1**	−1.14
2			−5	0.988	0.003	2.35	3.09	**1**	1.38
3	1.7	toluene	0	0.992	0.004	2.61	2.99	**1**	−0.09
4	1.7	toluene	20	0.987	0.007	2.52	2.88	**1**	0.03
5	1.7	CH_2Cl_2	20	0.996	0.173	3.21	0.91	**1**	0.01
6	6.9	toluene	20	0.985	0.006	2.44	2.97	**1**	1.30
7	4.5	toluene	40	0.984	0.008	2.56	3.00	**1**	−1.99
8	4	*n*-pentane	40	0.987	0.012	2.69	2.74	**1**	−2.94
9	4	*n*-pentane	52	0.986	0.023	2.75	2.42	**1**	−4.28
10	4	*n*-pentane	60	0.987	0.033	2.86	2.23	**1**	−8.40
11			60	1	0.394	"inf"	0.28	**1b**	8.00
12			60	1	0.439	"inf"	0.16	**1b**	8.00
13	6	toluene	80	0.987	0.004	3.04	3.79	**1**	0.00

[a] Taken from ref 11. [b] Defined as {[*mmmr*] + [*rrrm*] + 2[*mrrm*] } − {[*mmrm*] + [*rmrr*] + 2[*mmrr*]} (see eq 3).

studied in the presence of $MeB(C_6F_5)_3^-$ as the anion. The anion, initially closely interacting with the metal, is displaced to make room for the propylene, eventually forming a loose ion pair with the π complex. As can be seen from Figure 8, the approximate transition state for the trans uptake of propylene is approximately 10 kcal/mol higher than that for the cis uptake. Because of this large energy difference, for this system the contribution of the back-side attack to the *c* term can be neglected. Considering that the back-side attack is not as likely a source for *m* error dyads as the site epimerization, insertion and ion-pair formation are the two moments in the catalytic cycle where it is most likely an error can be produced.

It is also possible to calculate the parameters *a* and *c* from the experimental pentad distribution. In order to obtain reliable values of the parameters, very accurate experimental results are required, which must have the smallest possible deviation from the stoichiometric relationship[11]

$$[mmmr] + [rrrm] + 2[mrrm] = [mmrm] + [rmrr] + 2[mmrr] \quad (3)$$

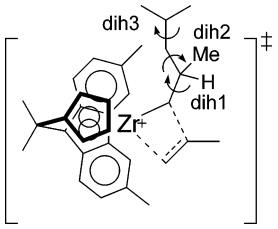

Figure 9. Dihedral angles studied in the systematic search of the propylene insertion TS rotamers.

Calculation of enantioface selectivities and of site epimerization energy barriers has been performed for several systems, using Farina's model.[11] Transition state theory then allows calculating the $\Delta\Delta G^{\ddagger}$ for the enantiomeric misinsertion (from *a*) and the site epimerization (from *c*). The experimental activation free energies depend, of course, in a complex way on the experimental conditions; however, on the average they are remarkably close to the computed activation energy values. Unfortunately, the data for the experimental pentad distribution obtained with **2b** are not reliable, as indicated by the large deviation from the stoichiometric relationship. Therefore, the experimental $\Delta\Delta G^{\ddagger}$ and the computed $\Delta\Delta E^{\ddagger}$ values cannot be compared.

Influence of Chain End Control on the Enantioface Selectivity. Although catalytic site control is the most important factor in determining enantioface selectivity, it cannot be ruled out a priori that the configuration of the stereogenic carbon, which is closest to the growing center (the chain end), does not play any role. Enantioface selectivities are expected to vary when the configuration at the chain end is R or S. Such a difference measures the importance of the chirality of the chain end in enantioface selectivity.

To investigate the issue, **2a** has been studied with a longer alkyl chain, obtained after two 1,2-propylene insertions. An alkyl chain this long contains a stereocenter at the chain end. Due to the increased length of the alkyl chain, for each of the four main conformations of the insertion transition state, several possible rotamers can exist. In order to determine the selectivity with such a long alkyl chain, it is necessary to explore systematically the conformational space of the transition states.

Table 8. Relative Energies (in kcal/mol) and Values of the Dihedral Angles (deg) of the Propylene Insertion Transition States, Explored to Assess the Influence of Chain End Control[a]

	insertion TS											
	previous correct insertion (S−C)						previous misinsertion (R−C)					
	CI (1,2-re)			EMI (1,2-si)			CI (1,2-re)			EMI (1,2-si)		
conf no.	S1a	S2a	S3a	S1a	S2a	S3a	R1a	R2a	R3a	R1a	R2a	R3a
dih 1	−135	−138	−138	−132	−133		100	109	100	107	104	
dih 2	171	59	−69	180	−67		−86	178	64	61	173	
dih 3	59	−56	36	62	35		43	23	−27	4	25	
E_{rel}	0 (0)	0.3	3.4	−1.7 (−1.4)	1.9		1.0	2.0	3.5	1.1 (1.0)	2.2	
conf no.	S1b	S2b	S3b	S1b	S2b	S3b	R1b	R2b	R3b	R1b	R2b	R3b
dih 1	−88	−88	−82	117	118		−137	−136	−147		−136	−138
dih 2	177	−51	−61	−178	55		−109	−178	56		−174	−65
dih 3	64	51	29	59	−59		52	24	−47		24	51
E_{rel}	−3.3	−0.3	0.1	−0.2	−0.1		−2.0	−2.1 (−2.2)	−0.9		6.1	3.6
conf no.	S1c	S2c	S3c	S1c	S2c	S3c	R1c	R2c	R3c	R1c	R2c	R3c
dih 1	104	109		−127			−104	*−120*	−129		−89	
dih 2	−83	170		−178			−58	*180*	71		173	
dih 3	30	59		67			56	*32*	−28		25	
E_{rel}	7.2*	2.8		−1.1			−2.4	*−0.8*	−0.7		2.6	
conf no.	S1d	S2d	S3d	S1d	S2d	S3d	R1d	R2d	R3d	R1d	R2d	R3d
dih 1	−159	180	−178	170	*147*	179	166	155	153	155	179	175
dih 2	−71	173	72	−179	*78*	−65	−72	179	68	69	−174	−67
dih 3	26	62	−44	67	*−50*	35	56	28	−28	−9	25	48
E_{rel}	3.8	0.9	1.1[b]	1.6	*0.3*	4.9	0.8	−0.2	0.5	5.3	5.1[b]	2.4
conf no.	S1e	S2e	S3e	S1e	S2e	S3e	R1e	R2e	R3e	R1e	R2e	R3e
dih 1		−13		−6				10			14	
dih 2		172		179				−157			−173	
dih 3		61		64				−48			24	
E_{rel}		−4.3 (−4.3)		3.8				0.4			1.6	

[a]Conformation CI (1,2-re)-S1a has been chosen arbitrarily as the reference state. Energy values obtained with single-point calculations in toluene solution are reported in parentheses. [b] C−C coupling distance constrained to typical values (2.2−2.3 Å).

The rotations along three dihedral angles have been explored systematically, as shown in Figure 9. For the correct 1,2-re insertion, the alkyl chain and the propylene monomer unit have been oriented in the "away/anti" conformation, which has been shown to be the most favorable channel. In the case of the misinsertion, the alkyl chain and propylene have been oriented as in the "toward/anti" conformation. With the position of the first two carbon atoms of the chain held fixed (which defines whether the chain is "toward" or "away"), rotation along the next two dihedral angles (dih1 and dih2, as shown in Figure 8) was explored systematically, at intervals of around 60° for dih1 and 120° for dih2. The orientation of the terminal i-Pr group is determined by the dihedral angle dih3, and it has been selected, as it seemed best to reduce repulsive interactions; some rotamers have not been optimized, because it seemed obvious that they are high-energy structures, due to considerable strain.

The energies of the gas-phase optimized transition states, together with the values of the three dihedral angles that define them, are reported in Table 8.

In the gas phase, the enantioface selectivity after a previous correct insertion is 2.6 kcal/mol, very similar to that obtained for **2a**, with only isobutyl as a model for the growing chain (see Table 1). The selectivity computed in the case of a previous stereoerror (which can be a misinsertion or a site epimerization) is slightly higher, at 3.0 kcal/mol. In toluene solution, the enantioface selectivity increases, consistently with the results previously reported in Table 2. The selectivity in toluene is 2.9 kcal/mol after a correct insertion and 3.2 kcal/mol after a stereoerror is produced. Because the enantioface selectivity increases after a stereoerror, the occurrence of two consecutive stereoerrors is extremely unlikely and the correct stereochemical sequence is restored. In this case, the chain end and the enantiomorphic catalyst site exert a matching influence on stereochemistry.

While it is evident that the configuration of the nearest stereogenic carbon has an influence on the stereochemistry of insertion, it is quite unlikely that it affects noticeably the dynamics of ion-pair formation.[70] The effect of chain end stereochemistry on site epimerization has therefore not been investigated.

Conclusions

Through this DFT study, we have explored the most likely mechanisms for the generation of stereoerrors in the syndiospecific polymerization of propylene with a C_s-symmetric system. The generation of stereodefects is described satisfactorily well when taking into account only misinsertions and site epimerization events as possible sources of stereoerrors.

Although it is known that the correct computational description of the overall reaction mechanism requires the explicit inclusion of the counteranion and of solvent effects, the counteranion and the solvent do not play a major role in the stereochemistry of insertion, due to the fact that charge separation in the insertion TS is roughly independent of the conformation. Differential solvation of the various insertion TS conformations also exerts a negligible influence on stereoselectivity. On the other hand, anion assistance is necessary for site epimerization to compete with propagation; therefore, including the anion explicitly is mandatory in this case. Solvation also plays a major role in the site epimerization. Calculations that do not include solvation effects are incapable of producing results that agree even qualitatively with experiments. The reassociation of the anion and the cation (both in the regular

propagation and in the site epimerization) is highly exothermic, which makes the site epimerization an irreversible process. Increasing the bulk of the anion reduces the incidence of site epimerization, both in the gas phase and in solution. Electrostatic interaction with the solvent is stronger when the anion and the cation are separated. Therefore, differential solvation increases the barrier to site epimerization, compared to the gas phase, especially for those species, such as Marks' fluoroaluminate, in which the anion charge is less dispersed.

The nature of the ligand system influences both the enantioface selectivity and the propensity to site epimerization. It has been found, in agreement with the experiment, that C_s-symmetric systems bearing a carbon bridge are more stereoselective and suffer less from site epimerization than systems having a Si bridge. The addition of substituents in the 3,6-positions of the fluorenyl moiety is also very beneficial for the suppression of misinsertion events, while it has a more subtle effect on the minimization of the site epimerization.

Using a two-parameter statistical scheme, it is possible to predict pentad distributions from the computational results on misinsertion and site epimerization with satisfactory accuracy. The chirality of the last generated stereocenter has also some influence on stereoselectivity. The chain end control, however, is not as important as the enantiomorphic site control. Its main effect is that resuming the correct stereochemical sequence after a stereoerror is favored because enantioface selectivity increases after the occurrence of a stereoerror.

Acknowledgment. This work has been supported financially by Total. T.Z. thanks the Canadian government for a Canada Research Chair in theoretical inorganic chemistry. Most of the calculations required for this research have been carried out using the WestGrid computing resources.

OM060786V